ELSEVIER

www.elsevier.nl/locate/jorganchem

Journal of Organometallic Chemistry 205 (2000) 193–201

Journal of Organo metallic Chemistry

Organometallic complexes for nonlinear optics[☆] Part 19. Syntheses and molecular quadratic hyperpolarizabilities of indoanilino–alkynyl–ruthenium complexes

Andrew M. McDonagh [a], Marie P. Cifuentes [a], Nigel T. Lucas [a], Mark G. Humphrey [a,*], Stephan Houbrechts [b], André Persoons [b]

[a] *Department of Chemistry, Australian National University, Canberra, ACT 0200, Australia*
[b] *Laboratory for Chemical and Biological Dynamics, University of Leuven, Celestijnenlaan 200D, B-3001 Leuven, Belgium*

Received 19 April 2000; accepted 18 May 2000

Abstract

The terminal alkyne $4\text{-HC}{\equiv}\text{CC}_6\text{H}_4\text{N}{=}\text{CCH}{=}\text{C}^t\text{BuC(O)C}^t\text{Bu}{=}\text{CH}$ (**1**) and ruthenium complex derivatives *trans*-$[\text{Ru}(\text{C}{\equiv}\text{C-4-C}_6\text{H}_4\text{N}{=}\text{CCH} = \text{C}^t\text{BuC(O)C}^t\text{Bu}{=}\text{CH})\text{Cl}(\text{dppm})_2]$ (**2**) and $[\text{Ru}\{\text{C}{\equiv}\text{C-4-C}_6\text{H}_4\text{N}{=}\text{CCH}{=}\text{C}^t\text{BuC(O)C}^t\text{Bu}{=}\text{CH}\}(\text{PPh}_3)_2(\eta\text{-C}_5\text{H}_5)]$ (**3**) have been synthesized. An X-ray structural study of **3** reveals the expected equivalent C–C bond lengths of the phenyl and alternating C–C and C=C bond lengths of the quinonal ring in the indoanilino–alkynyl ligand; there is a dihedral angle of 47.59° between the phenyl and quinonal rings, probably a result of *ortho*-hydrogen repulsion. Metal-centred oxidation potentials of **2** and **3** are similar to those of 'extended chain' 4-nitroaryl–alkynyl complex analogues. Irreversible quinonal ring-centred reductions occur at significantly more negative potentials than the quasi-reversible reductions in their nitro-containing analogues. Quadratic optical nonlinearities by hyper-Rayleigh scattering at 1064 nm for **2** (417×10^{-30} esu) and **3** (658×10^{-30} esu) are both large, but resonance enhanced. Two-level-corrected nonlinearities for these complexes (124×10^{-30}, 159×10^{-30} esu, respectively) are also large, despite the presence of electron-donating *tert*-butyl groups reducing the efficiency of the (formally) electron-accepting quinonal ring in these donor-bridge-acceptor complexes. © 2000 Elsevier Science S.A. All rights reserved.

Keywords: Ruthenium; X-ray structure; Electrochemistry; Quadratic hyperpolarizabilities; Alkynyl; Nonlinear optics

1. Introduction

The quadratic and cubic nonlinear optical (NLO) properties of organometallic complexes have come under intense scrutiny recently [2–6]. The most successful class of compounds for quadratic NLO merit are those coupling an electron-rich donor to an electron-poor acceptor by means of a π-delocalizable bridging unit. Aryl–alkynyl complexes with a donor-bridge-acceptor composition such as *trans*-$[\text{Ru}(\text{C}{\equiv}\text{CC}_6\text{H}_4\text{NO}_2\text{-4})\text{Cl}(\text{dppm})_2]$ are amongst the most efficient organometallic quadratic NLO materials [7]. However, although the aryl–alkynyl π-bridge linking the electron-rich ligated metal donor to the nitro acceptor affords robust metal complexes, it is not necessarily the most effective bridge for maximizing NLO merit. This can be understood by considering the perturbation theory-derived expression for NLO responses, in which a charge-separated excited state is mixed into the ground state of the molecule. For complexes such as *trans*-$[\text{Ru}(\text{C}{\equiv}\text{CC}_6\text{H}_4\text{NO}_2\text{-4})\text{Cl}(\text{dppm})_2]$, the charge-separated excited state is energetically disfavoured by the loss of aromatic stabilization energy in proceeding from the aromatic ground state to the quinonal-like charge separated excited state (Fig. 1(a)); the excited state consequently mixes less with the ground state, resulting in a less-efficient NLO material than would otherwise be achievable.

This problem has been addressed with organic molecules. In the search for efficient organic NLO materials, attention has turned to indoanilines [8,9], in

---

[☆] For Part 18, see Ref. [1].

* Corresponding author. Tel.: +61-2-62492927; fax: +61-2-62490760.

E-mail address: mark.humphrey@anu.edu.au (M.G. Humphrey).

0022-328X/00/$ - see front matter © 2000 Elsevier Science S.A. All rights reserved.
PII: S0022-328X(00)00312-0

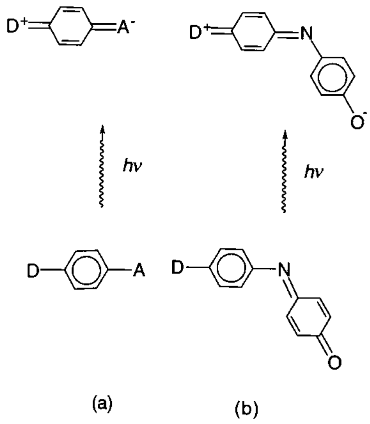

Fig. 1. (a) Ground and CT excited states of donor(D)-acceptor aryl compounds. (b) Ground and CT excited states of indoaniline compounds.

which an arylene group is connected to a quinonal group via a nitrogen atom. In the ground state, there is one aromatic ring and one quinonal ring. Upon excitation, this system compensates for the loss in aromaticity of the aromatic ring by the gain of aromaticity of the quinonal ring (Fig. 1(b)). As a consequence, organic compounds with this composition are efficient NLO materials.

No transition metal complexes bearing this type of substituent have thus far been reported. This paper reports the preparation of the new alkyne $4\text{-HC}{\equiv}\text{CC}_6\text{H}_4\text{N}{=}\overline{\text{CCH}{=}\text{C}^t\text{BuC(O)C}^t\text{Bu}{=}\text{C}}\text{H}$, its use in the preparation of indoanilino–alkynyl–ruthenium complexes, an X-ray structural study of a representative complex, electrochemical data and quadratic NLO data for the new compounds, and comparison of their efficiency with previously reported aryl–alkynyl complexes.

2. Results and discussion

2.1. Synthesis and characterization of $4\text{-HC}{\equiv}\text{CC}_6\text{H}_4\text{N}{=}\overline{\text{CCH}{=}\text{C}^t\text{BuC(O)C}^t\text{Bu}{=}\text{C}}\text{H}$ (1)

The preparation of the new alkyne (**1**) follows the procedure outlined in Scheme 1(a). The iodide $4\text{-IC}_6\text{H}_4\text{N}{=}\overline{\text{CCH}{=}\text{C}^t\text{BuC(O)C}^t\text{Bu}{=}\text{C}}\text{H}$ was obtained in good yield by employing two modifications to the literature procedure for preparing indoanilines [10]: (i) an excess of 4-iodoaniline was used to ensure the complete reaction of 2,6-di-*tert*-butylbenzoquinone and to simplify the purification of the product (the product is difficult to separate from 2,6-di-*tert*-butylbenzoquinone by column chromatography, but is readily separated from the excess 4-iodoaniline), and (ii) the boron trifluoride catalyst was replenished periodically over the course of the reaction (without this periodic addition, the reaction will not proceed further). Sonogashira coupling [11] was then employed to obtain the terminal alkyne **1** in moderate yield. No advantage in purity or yield of the final product was gained by isolating the intermediate trimethylsilyl-protected alkyne prior to the deprotection step. An alternative synthesis involving the coupling of trimethylsilylethyne to 4-iodoaniline followed by reaction of the resulting 4-trimethylsilylethynylaniline with 2,6-di-*tert*-butylbenzoquinone (Scheme 1(b)) afforded a lower yield of **1**, along with several unidentified by-products.

The ^{1}H-NMR spectra of the new indoaniline compounds are particularly informative. The ^{1}H-NMR spectrum of the iodo-containing intermediate, $4\text{-IC}_6\text{H}_4\text{N}{=}\overline{\text{CCH}{=}\text{C}^t\text{BuC(O)C}^t\text{Bu}{=}\text{C}}\text{H}$, contains a characteristic AA′BB′ pattern centred on 7.16 ppm and assigned to the protons on the aromatic ring. Restricted rotation about the C=N bond results in inequivalent quinone ring protons (doublet signals at 7.01 and 6.74 ppm) and inequivalent *tert*-butyl groups (singlet signals

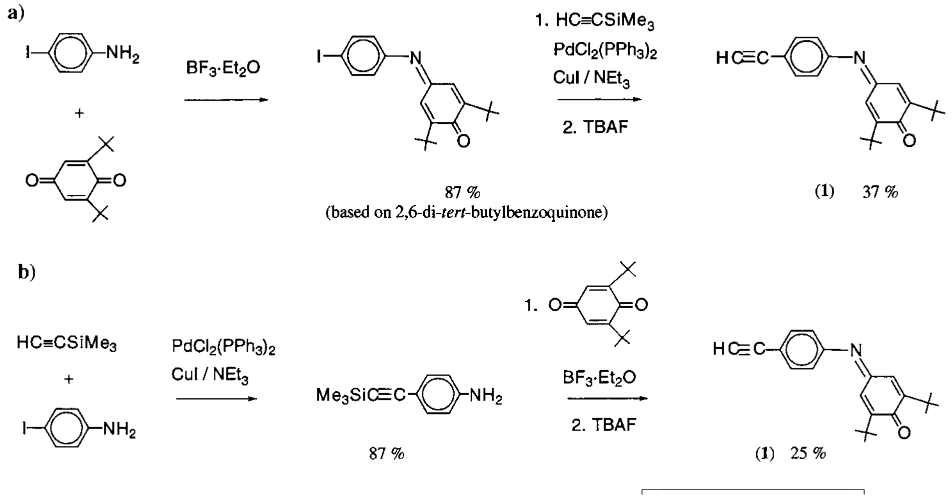

Scheme 1. Alternate routes for the preparation of $4\text{-HC}{\equiv}\text{CC}_6\text{H}_4\text{N}{=}\overline{\text{CCH}{=}\text{C}^t\text{BuC(O)C}^t\text{Bu}{=}\text{C}}\text{H}$) (**1**).

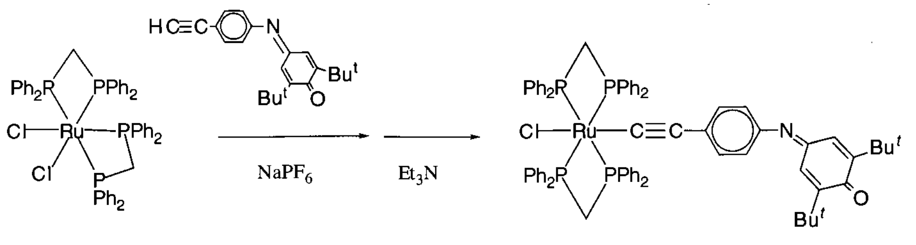

(**2**)

Scheme 2. Preparation of *trans*-[Ru(C≡C-4-$C_6H_4N{=}\overline{CCH{=}C^tBuC(O)C^tBu{=}C}H)Cl(dppm)_2$] (**2**).

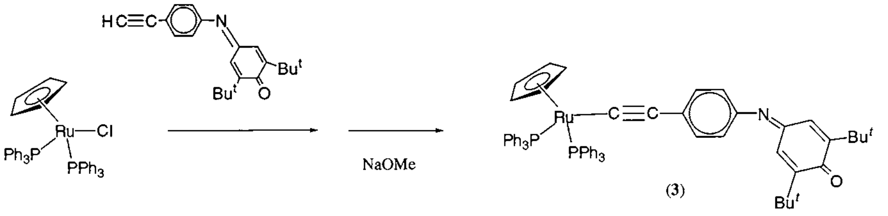

(**3**)

Scheme 3. Preparation of [Ru(C≡C-4-$C_6H_4N{=}\overline{CCH{=}C^tBuC(O)C^tBu{=}C}H)(PPh_3)_2(\eta\text{-}C_5H_5)$] (**3**).

at 1.30 and 1.18 ppm). The ^{1}H-NMR spectrum of the new alkyne **1** is similar to that of its precursor (quinone ring protons at 7.00 and 6.72 ppm, and *tert*-butyl protons at 1.31 and 1.17 ppm), and contains a characteristic signal assigned to the terminal alkyne proton at 3.10 ppm.

2.2. Synthesis and characterization of $L_nM\{C{\equiv}C\text{-}4\text{-}C_6H_4N{=}\overline{CCH{=}C^tBuC(O)C^tBu{=}C}H\}$ [L_nM = *trans*-[RuCl(dppm)$_2$] (**2**), Ru(PPh$_3$)$_2$(η-C$_5$H$_5$) (**3**)]

We have previously reported studies of quadratic NLO efficiencies of donor-π-bridge acceptor alkynyl–metal complexes with a range of ligated metal centres [7,12–15]; ruthenium-containing complexes are significantly more efficient than their nickel- or gold-containing analogues. It is sensible to employ the most efficient donor when evaluating acceptor groups. We have consequently prepared alkynyl–ruthenium derivatives of **1** with ligand sets shown to afford highly efficient quadratic NLO materials in our earlier work.

The syntheses of alkynyl complexes **2** (Scheme 2) and **3** (Scheme 3) follow the literature procedures of Dixneuf [16] and Bruce [17], respectively, for the preparation of the phenyl–alkynyl complex analogues. Reaction of *cis*-[RuCl$_2$(dppm)$_2$], sodium hexafluorophosphate and the terminal alkyne in dichloromethane at room temperature (r.t.) afforded *trans*-[Ru{C=CH-4-$C_6H_4N{=}\overline{CCH{=}C^tBuC(O)C^tBu{=}C}H$}Cl(dppm)$_2$]PF$_6$. This product was not isolated, but instead deprotonated with base in situ (using either sodium methoxide or triethylamine) to afford the desired alkynyl complex **2** in good yield (65%). Reaction of [RuCl(PPh$_3$)$_2$(η-C$_5$H$_5$)] with the terminal alkyne in refluxing methanol afforded the vinylidene complex [Ru{C=CH-4-$C_6H_4N{=}\overline{CCH{=}C^tBuC(O)C^tBu{=}C}H$}(PPh$_3$)$_2$($\eta$-C$_5H_5$)]$^+$; unlike the chlorobis(dppm)ruthenium–vinylidene complex above, the cyclopentadienylbis(triphenylphosphine)ruthenium analogue does not require the presence of large counter-ions (such as hexafluorophosphate) for stability, the displaced chloride presumably being sufficient. This vinylidene complex was similarly deprotonated in situ to afford **3** in 32% yield.

The new alkynyl complexes were characterized by FAB mass spectrometry, UV–vis, IR, ^{1}H-, ^{31}P- and ^{13}C-NMR spectroscopy. The FAB mass spectra of **2** and **3** contain molecular ions, with fragmentation of the former proceeding by competitive loss of chloro and alkynyl ligands to afford the base peak corresponding to [Ru(dppm)$_2$]$^+$, and fragmentation of the latter proceeding by competitive loss of phosphine and alkynyl ligand to afford the base peak corresponding to [Ru(PPh$_3$)(η-C$_5$H$_5$)]$^+$. The IR spectra contain characteristic bands assigned to ν(C≡C) at 2067 (**2**) and 2061 (**3**) cm^{-1}. The ^{31}P-NMR spectra contain singlet resonances at -6.1 (**2**) and 50.7 (**3**) ppm, with that of the former confirming the mutually *trans* stereochemistry of the chloro and alkynyl ligands. The ^{1}H-NMR spectra contain the above-mentioned characteristic signals from the quinonal rings. The ^{13}C-NMR spectra contain downfield resonances at 187.8 (**2**) and 187.9 (**3**) ppm corresponding to the quinonal carbon atoms. Complexes **2** and **3** both show a small positive solvatochromatic response with their electronic absorption spectra maxima in proceeding from solvent cyclohexane (λ_{max} **2** 637, **3** 613 nm) to solvent methanol (λ_{max} **2** 640, **3** 619 nm).

Table 1
Selected structural data for [Ru(C≡C-4-C_6H_4N=CCH=C^{t}BuC(O)C^{t}Bu=CH)$(PPh_3)_2$(η-C_5H_5)] (**3**)

Ru(1)–P(1)	2.309(2)
Ru(1)–P(2)	2.292(2)
Ru(1)–C(1)	2.010(7)
C(1)–C(2)	1.200(9)
C(2)–C(3)	1.43(1)
C(3)–C(4)	1.41(1)
C(3)–C(8)	1.41(1)
C(4)–C(5)	1.38(1)
C(7)–C(8)	1.38(1)
C(5)–C(6)	1.40(1)
C(6)–C(7)	1.40(1)
C(6)–N(1)	1.40(1)
N(1)–C(9)	1.28(1)
C(9)–C(10)	1.47(1)
C(9)–C(14)	1.46(1)
C(10)–C(11)	1.33(1)
C(13)–C(14)	1.34(1)
C(11)–C(12)	1.50(1)
C(12)–C(13)	1.49(1)
C(12)–O(1)	1.21(1)
Ru(1)–C(1)–C(2)	175.4(6)
C(1)–C(2)–C(3)	168.8(8)
C(6)–N(1)–C(9)	122.2(8)

2.3. X-ray structural study of [Ru(C≡C-4-C_6H_4N=CCH=C^{t}BuC(O)C^{t}Bu=CH)$(PPh_3)_2$-(η-C_5H_5)] (3)

We have completed an X-ray diffraction study of **3** to confirm the molecular composition. Important bond lengths and angles are given in Table 1 and an ORTEP plot is displayed in Fig. 2.

Ru–P and Ru–C(Cp) distances and intraphosphine and intracyclopentadienyl bond lengths and angles are unexceptional [18]. The Ru–C(alkynyl) and C≡C distances are also similar to literature precedents, with the deviation from linearity of the Ru–C≡C and C≡C–C linkages presumably due to packing effects. The bond distances within the indoanilino phenyl and quinonal rings are those expected for the ground-state structure, namely a bond-equalized phenyl group and bond-alternated quinonal moiety. The phenyl and quinonal rings are significantly removed from coplanarity (dihedral angle 47.59°) consistent with previous work with organic indoanilines by Marder et al. [8] where steric interactions between *o*-hydrogens were proposed to preclude coplanar indoaniline rings.

2.4. Electrochemical studies

The results of cyclic voltammetric studies on the alkynyl complexes **2** and **3** are summarized in Table 2, together with previously reported data for related complexes.

We have previously noted that (i) ruthenium is oxidized at potentials 0.2 V higher upon replacement of C≡CPh by 4-C≡C$C_6H_4NO_2$ (proceeding from **8** or **9** to **4** or **5**, respectively), and that (ii) a significant decrease in potential of the $Ru^{II/III}$ couple (0.16–0.18 V) is observed on 'chain-lengthening' the acetylide ligand from 4-C≡C$C_6H_4NO_2$ to 4-C≡CC_6H_4-(*E*)-CH=CH-4-$C_6H_4NO_2$ in proceeding from **4** or **5** to **6** or **7**, respectively [14]. In this work substitution of the 4-NO_2 moiety by the 4-N=CCH=C^{t}BuC(O)C^{t}Bu=CH group results in a decrease of 0.19 V (proceeding from **5** to **3**) or 0.23 V (from **4** to **2**). Thus, the indoanilinoalkynyl

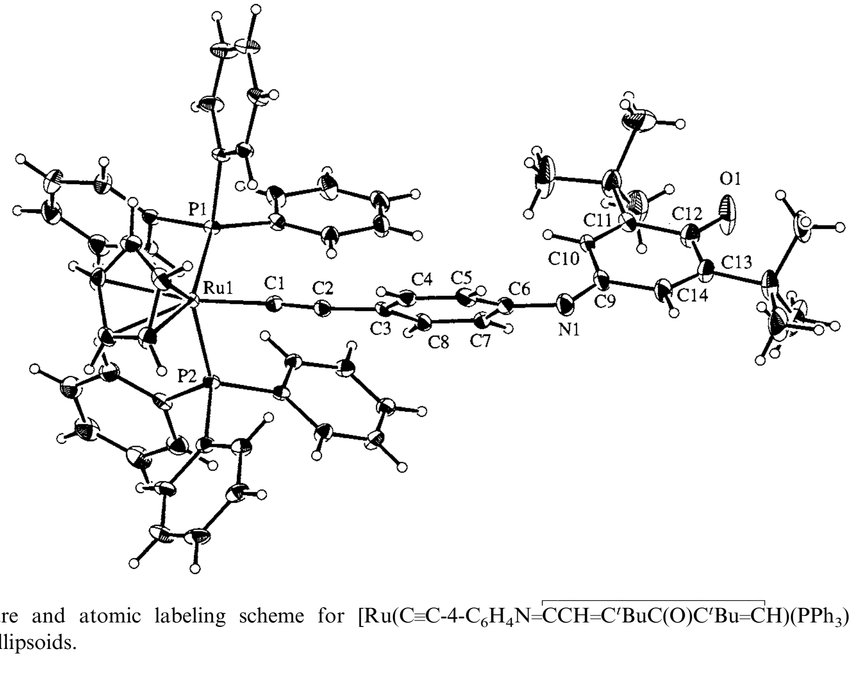

Fig. 2. Molecular structure and atomic labeling scheme for [Ru(C≡C-4-C_6H_4N=CCH=C^{t}BuC(O)C^{t}Bu=CH)$(PPh_3)_2$(η-C_5H_5)] (**3**) with 20% anisotropic displacement ellipsoids.

Table 2
Cyclic voltammetric, linear optical and quadratic nonlinear optical response parameters for indoanilino–alkynyl–ruthenium complexes and related compounds

Compound	$E^0_{\mathrm{Ru^{II/III}}}$ (V) [i_{pc}/i_{pa}]	$E^0_{\mathrm{A^{0/-I}}}$ (V) [i_{pa}/i_{pc}]	λ_{max} (nm) [ε (10^4 M^{-1} cm^{-1})]	β (10^{-30} esu) [a]	β_0 (10^{-30} esu) [b]	Ref.
4-HC≡CC$_6$H$_4$N=CCH=C^{t}BuC(O)C^{t}Bu=CH (**1**)			448 (0.5)	[b]		This work
4-HC≡CC$_6$H$_4$NO$_2$			288 (1.5)	14 [c]	9 [d]	[13]
4-HC≡CC$_6$H$_4$-(*E*)-CH=CH-4-C$_6$H$_4$NO$_2$			358 (3.3)	55 [c]	27 [d]	[13]
trans-[Ru{C≡C-4-C$_6$H$_4$N=CCH=C^{t}BuC(O)C^{t}Bu=CH}Cl(dppm)$_2$] (**2**)	0.49 (1.0)	−1.15 [h]	645 (0.8)	417 [c]	124 [d]	This work
trans-[Ru(C≡CPh)Cl(dppm)$_2$] (**8**)	0.55 (1.0)		308 (1.7)	20 [c]	12 [d]	[7]
trans-[Ru(C≡C-4-C$_6$H$_4$NO$_2$)Cl(dppm)$_2$] (**4**)	0.72 (0.9)	−1.08 (0.7)	473 (1.8)	767 [c]	129 [d]	[7]
trans-[Ru{C≡C-4-C$_6$H$_4$-(*E*)-CH=CH-4-C$_6$H$_4$NO$_2$}Cl(dppm)$_2$] (**6**)	0.56 (1.0)	−0.87 (0.4)	490 (2.6)	1964 [c]	235 [d]	[7]
[Ru{C≡C-4-C$_6$H$_4$N=CCH=C^{t}BuC(O)C^{t}Bu=CH}-(PPh$_3$)$_2$(η-C$_5$H$_5$)] (**3**)	0.54 (1.0)	−1.23 [h]	622 (1.6)	658 [c]	159 [d]	This work
[Ru(C≡CPh)(PPh$_3$)$_2$(η-C$_5$H$_5$)] (**9**)	0.55 (0.7)		310 (2.0)	16 [c]	10 [d]	[14]
[Ru(C≡C-4-C$_6$H$_4$NO$_2$)(PPh$_3$)$_2$-(η-C$_5$H$_5$)] (**5**)	0.73 (1.0)	−1.08 (1.0)	460 (1.1)	468 [c]	96 [d]	[12,14,19]
[Ru{C≡C-4-C$_6$H$_4$-(*E*)-CH=CH-4-C$_6$H$_4$NO$_2$}(PPh$_3$)$_2$(η-C$_5$H$_5$)] (**7**)	0.55 (0.9)	−0.92 (0.3)	476 (2.6)	1455 [c]	232 [d]	[12,14,19]
4-Me$_2$NC$_6$H$_4$N=CCH=CHC(O)CH=CH			590 [e]	190 [f]	106 [g]	[8]
4-$_2$NC$_6$H$_4$N=CCH=C^{t}BuC(O)C^{t}Bu=CH			558 [e]	78 [f]	47 [g]	[9]
4-Me$_2$NC$_6$H$_4$-(*E*)-CH=CH-4-C$_6$H$_4$N=CCH=C^{t}BuC(O)C^{t}Bu=CH			512 [e]	116 [f]	77 [g]	[9]

[a] All compounds are optically transparent at the fundamental frequencies.

[b] Response too low to measure.

[c] HRS at 1064 nm; values ± 10%, using *p*-nitroaniline ($\beta = 21.4 \times 10^{-30}$ esu) as a reference.

[d] Data corrected for resonance enhancement at 532 nm using the two-level model with $\beta_0 = \beta[1-(2\lambda_{max}/1064)^2][1-(\lambda max/1064)^2]$; damping factors not included.

[e] Molar absorptivity not reported.

[f] First hyperpolarizability measured by EFISH at 1.91 μm.

[g] Data corrected for resonance enhancement at 0.96 μm using the two-level model with $\beta_0 = \beta[1-(2\lambda_{max}/1910)^2][1-(\lambda_{max}/1910)^2]$.

[h] $E_{\mathrm{pc\ A^{0/-I}}}$ (V).

ligand has the same effect upon metal-centred oxidation potential as ‘chain-lengthening’ nitro-substituted aryl–alkynyl ligands. Unlike the nitro-centred reductions in **4**–**7** which are quasi-reversible, the reductions of the quinonal group in **2** and **3** are irreversible using a scan rate of 100 mV s^{-1}, with evidence of return peaks ($E_{pa} - E_{pc} = 0.9$ V) observed at higher scan rates (400–1000 mV s^{-1}). The oxidations are correlated with a metal-centred HOMO and the reductions with a quinonal-localized LUMO. Proceeding from 4-nitrophenyl–alkynyl complexes **4** and **5** to 4-indoanilino–alkynyl complexes **2** and **3**, respectively, results in a decrease in the energy difference between HOMO and LUMO, manifested in both an increase in λ_{max} and a decrease in $E^0_{\mathrm{Ru^{II/III}}} - E^0_{\mathrm{A^{0/-I}}}$; a similar result has been observed in proceeding from 4-nitrophenyl–alkynyl complexes **4** and **5** to 4,4′-(*E*)-nitrostilbenylalkynyl complexes **6** and **7** [14].

2.5. Nonlinear optical studies

Quadratic optical nonlinearities of the new compounds were determined using the hyper-Rayleigh scattering technique at 1064 nm. The results of these studies are given in Table 2, together with linear optical absorption data, and results for related ruthenium complexes and organic indoanilines for comparison.

The two-level model, which was developed to explain the quadratic NLO merit of simple donor-bridge-acceptor organics, assumes that the dominant contribution to β is associated with the charge-transfer transition along the molecular dipole axis. The β_{CT} (β in the direction of the charge-transfer axis) is then given by:

$$\beta_{CT} \alpha \frac{\mu_{eg}^2(\mu_e - \mu_g)\omega_{eg}^2}{(\omega_{eg}^2 - \omega^2)(\omega_{eg}^2 - 4\omega^2)}$$

where ω_{eg} is the ground to excited state transition energy (which can be obtained from λ_{max} in the electronic absorption spectrum), μ_{eg} is the transition dipole moment (obtained from integration of the absorption band in the UV–vis spectrum), and μ_g and μ_e are the ground state and the excited state dipole moments. The applicability of this model to donor-bridge-acceptor organometallics is questionable (it is likely more than one transition may be important for β in complex molecules). This model suggests that the quadratic NLO coefficient should be increased upon red-shifting the optical absorption band, and upon increasing the intensity of this transition. The optical absorption maximum for the indoanilino–alkynyl–ruthenium complexes prepared in the current study are significantly red-shifted compared to those of related nitroaryl–alkynyl complexes [18,20]; whereas the latter complexes are red in colour, the former complexes are blue. However, the intensity of this MLCT transition is significantly weaker for the indoanilino–alkynyl–ruthenium complexes.

The optical nonlinearities of the new complexes are resonance enhanced due to the proximity of the optical absorption frequency to the second-harmonic frequency. Assuming that the dominant contribution to resonance enhancement arises from the charge-transfer transition (as in the present complexes), it is possible to apply a two-level correction to the experimental data to afford approximated zero-frequency nonlinearities β_0. The shortcomings of this approach when applied to organometallics have been discussed elsewhere [5], but this procedure arguably provides a useful way to compare resonance-enhanced data and afford qualitative insights. To facilitate comparisons of quadratic NLO merit in the present study, two-level-corrected nonlinearities are also presented.

The quadratic nonlinearity of the new organic alkyne was too low to measure. In contrast, experimental β values of the indoanilino–alkynyl–ruthenium complexes **2** and **3** are both large. As with the related complexes bearing 4-nitrophenylalkynyl (**4**, **5**) or 4,4′-(*E*)-nitrostilbenylalkynyl ligands (**6**, **7**) (Table 2), complexes **2** and **3** can be viewed as (conceptual) derivatives of their phenylalkynyl analogues (**8**, **9**). Introduction of acceptor substituent in proceeding from phenyl–alkynyl complex (**8**, **9**) to indoanilino–alkynyl analogue (**2**, **3**) results in significant increases in both experimentally obtained and two-level-corrected nonlinearities (Table 2). Complex **3** has larger β_{exp} and β_0 values than its 4-nitrophenylalkynyl analogue **5**. However, the opposite trend is observed for β_{exp} for **2** and its 4-nitrophenylalkynyl analogue **4**, and β_0 for these complexes are equivalent within experimental error; from the perspective of β normalized for chromophore chain length, the complexes with the 4-nitrophenylalkynyl ligand are the more efficient. Comparison of **2** and **3** with their 4,4′-(*E*)-nitrostilbenylalkynyl analogues (**6**, **7**), which have a similar chromophore chain length, reveals that the latter possess much larger β_{exp} and β_0 coefficients.

The 4,4′-(*E*)-nitrostilbenylalkynyl complexes **6** and **7** have some of the largest quadratic optical nonlinearities observed thus far for organometallic complexes. The presence of the indoanilinoalkynyl ligands in **2** and **3** might have been expected to afford complexes with similarly large nonlinearities. The lower-than-expected β values recorded for **2** and **3** may be due to both steric and electronic factors. The structural study above confirms that steric repulsion between the *ortho*-hydrogens of the indoanilino–alkynyl ligand phenyl and quinonal rings results in a lack of coplanarity which will disfavour extensive π-delocalization. The presence of electron-rich *tert*-butyl groups may reduce the electron acceptor properties of the quinone ring. The electronic factor has been noted previously with organic compounds [9]. Quadratic nonlinearity β was reduced by a factor of two or more on proceeding from $4,4'\text{-}Me_2NC_6H_4N{=}\overline{CCH{=}C^tBuC(O)C^tBu{=}C}H$ to the di-*tert*-butylated compound $4,4'\text{-}Me_2NC_6H_4N{=}\overline{CCH{=}C^tBuC(O)C^tBu{=}C}H$. Although synthetic considerations have so far necessitated the inclusion of the *tert*-butyl groups in our organometallic complexes, these observations in the organic system suggest that a similar ligand without *tert*-butyl groups should afford complexes with very large two-level-corrected nonlinearities.

3. Experimental

3.1. General

All reactions were performed under a nitrogen atmosphere with the use of Schlenk techniques unless otherwise stated. Dichloromethane was dried by distilling over CaH_2, methanol was dried by distilling over $Mg–I_2$, and tetrahydrofuran was dried by distilling over sodium–benzophenone; other solvents were used as received. 'Pet. spirit' refers to a fraction of petroleum ether of boiling range 60–80°C. Chromatography was on silica gel (230–400 mesh ASTM) or ungraded basic alumina.

$[RuCl(PPh_3)_2(\eta\text{-}C_5H_5)]$ [21] and *cis*-$[RuCl_2(dppm)_2]$ [22] were prepared by the literature procedures. Sodium methoxide solutions were prepared by reacting sodium with dry methanol. Bis(triphenylphosphine)-palladium(II) chloride was prepared by stirring two equivalents of triphenylphosphine with palladium(II) chloride in dimethylformamide at reflux for 2 h. The resulting precipitate was collected and recrystallized from chloroform. Sodium hexafluorophosphate (Aldrich) was recrystallized from acetonitrile before use. 2,6-Di-*tert*-butyl-1,4-benzoquinone (Aldrich), 4-

iodoaniline (Aldrich), boron trifluoride etherate (Aldrich), trimethylsilylethyne (Aldrich), copper(I) iodide (Unilab), tetrabutylammonium fluoride (1 M solution in tetrahydrofuran) (Aldrich), sulfuric acid (98%) (Univar), and anhydrous magnesium sulfate (Aldrich) were used as received.

EI (electron impact) mass spectra (both unit resolution and high resolution (HR)) were recorded using a VG Autospec instrument (70 eV electron energy, 8 kV accelerating potential) and secondary ion mass spectra were recorded using a VG ZAB 2SEQ instrument (30 kV Cs^+ ions, current 1 mA, accelerating potential 8 kV, 3-nitrobenzyl alcohol matrix) at the Research School of Chemistry, Australian National University; peaks are reported as m/z (assignment, relative intensity). Microanalyses were carried out at the Research School of Chemistry, Australian National University. IR spectra were recorded as dichloromethane solutions using a Perkin–Elmer System 2000 FTIR. UV–vis spectra reported below and in Table 2 were recorded using either a Cary 4 or Cary 5 spectrophotometer of solutions in THF in 1 cm cells (additional spectra for solvatochromic studies summarized in Section 2 were obtained under similar conditions in cyclohexane and methanol). ^1H- (300 MHz), ^{13}C- (75 MHz) and ^{31}P- (121 MHz) NMR spectra were recorded using a Varian Gemini-300 FT NMR spectrometer in $CDCl_3$ and are referenced to residual solvent (^1H, ^{13}C) or external 85% H_3PO_4 (^{31}P). The assignments follow the numbering schemes shown in Fig. 3. Electrochemical measurements were recorded using a MacLab 400 interface and MacLab potentiostat from ADInstruments. The supporting electrolyte was 0.1 M $[N^nBu_4]$ $[PF_6]$ in distilled, deoxygenated CH_2Cl_2. Solutions containing ca. 1×10^{-3} M complex were maintained under nitrogen. Measurements were carried out using a platinum disc working, Pt auxiliary and Ag–AgCl reference electrode, such that the ferrocene–ferrocenium redox couple was located at 0.56 V. Scan rates were 100 mV s^{-1}.

3.2. Syntheses of indoanilines

3.2.1. $4\text{-}IC_6H_4N{=}\overline{CCH{=}C^tBuC(O)C^tBu{=}CH}$

A mixture of 2,6-di-*tert*-butyl-1,4-benzoquinone (500 mg, 2.27 mmol), 4-iodoaniline (1.40 g, 6.39 mmol) and boron trifluoride etherate (30 μl, 0.16 mmol) was stirred in tetrahydrofuran (30 ml) at reflux for 7 h with a further six aliquots of boron trifluoride etherate (30 μl) being added at hourly intervals. The mixture was then allowed to cool to r.t. and the solvent removed in vacuo. The residue was purified by silica column chromatography, the product being eluted with 3:5 dichloromethane–pet. spirit. Reduction of solvent volume on a rotary evaporator afforded the product as an orange powder (800 mg, 84% based on di-*tert*-butylbenzoquinone). HR MS (EI) $C_{20}H_{24}INO$: Anal. Calc. 421.0903, found 421.0906. ^1H-NMR (δ): 1.18 (s, 9H, Me_a), 1.30 (s, 9H, Me_b), 6.63 (d, $J_{HH} = 8$ Hz, 2H, H_5), 6.74 (d, $J_{HH} = 3$ Hz, 1H) 7.01 (d, $J_{HH} = 3$ Hz, 1H, H_{10}, H_{14}), 7.69 (d, $J_{HH} = 8$ Hz, 2H, H_4).

*3.2.2. $4\text{-}HC{\equiv}CC_6H_4N{=}\overline{CCH{=}C^tBuC(O)C^tBu{=}CH}$ (**1**)*

A mixture of $4\text{-}IC_6H_4N{=}\overline{CCH{=}C^tBuC(O)C^tBu{=}CH}$ (300 mg, 0.71 mmol), trimethylsilylethyne (0.40 ml, 2.8 mmol), bis(triphenylphosphine)palladium(II) chloride (5 mg, 0.007 mmol) and copper(I) iodide (5 mg, 0.03 mmol) was stirred in triethylamine (10 ml, deoxygenated) for 1 h. The solvent was removed in vacuo and the residue was dissolved in dichloromethane and passed through a plug of silica. The volume was reduced to around 20 ml, and a solution of tetrabutylammonium fluoride (1 ml, 1 M solution in tetrahydrofuran) was added with stirring. After 5 min, the solvent was removed and the residue purified by silica column chromatography. Concentration of solvent volume on a rotary evaporator afforded the product as an orange powder (85 mg, 37%). EI MS: 319 ($[M]^+$, 100), 304 ($[M-Me]^+$, 25). Anal. Calc. for $C_{22}H_{25}NO$: C, 82.72; H, 7.89; N, 4.38. Found: C, 82.48; H, 7.79; N, 3.89%. UV–vis (λ_{max}, nm [ε, M^{-1} cm^{-1}]): 448 [4700], 256 [28 000], 254 [15 000]. IR: ν(C=O) 1633 cm^{-1}. ^1H-NMR: δ 1.17 (s, 9H), 1.31 (s, 9H, Me_a, Me_b), 3.10 (s, 1H, HC≡C), 6.72 (d, $J_{HH} = 3$ Hz, 1H), 7.00 (d, $J_{HH} = 3$ Hz, 1H, H_{10}, H_{14}), 6.82 (d, $J_{HH} = 8$ Hz, 2H, H_4), 7.50 (d, $J_{HH} = 8$ Hz, 2H, H_5). ^{13}C-NMR: δ 29.4 (Me_a, Me_b), 35.4 (C_{16}), 35.8 (C_{15}), 77.5 (C_1), 83.4 (C_2), 118.9 (C_3), 120.8 (C_5), 132.8 (C_4), 121.3, 134.3 (C_{10}, C_{14}), 150.0 (C_6), 153.4, 154.2, 158.8 (C_9, C_{11}, C_{13}), 187.5 (C_{12}).

3.3. Syntheses of metal acetylide complexes

*3.3.1. Trans-$[Ru(C{\equiv}C\text{-}4\text{-}C_6H_4N{=}\overline{CCH{=}C^tBuC(O)C^tBu{=}CH})Cl(dppm)_2]$ (**2**)*

Cis-$[RuCl_2(dppm)_2]$ (140 mg, 0.16 mmol), $4\text{-}HC{\equiv}CC_6H_4N{=}\overline{CCH{=}C^tBuC(O)C^tBu{=}CH}$ (75 mg, 0.24 mmol) and sodium hexafluorophosphate (55 mg, 0.33 mmol) were stirred in dichloromethane (5 ml) for 5 h at r.t. Triethylamine (1 ml) was added with stirring and the solvent removed in vacuo after 1 min. The residue was adsorbed onto basic alumina and placed atop an alumina column. Elution with 1:3 dichloromethane–pet. spirit removed unreacted alkyne. The product was eluted with 4:1 dichloromethane–pet. spirit. Evaporation of the solvent on a rotary evaporator yielded 123 mg (65%) of a deep blue powder. FAB MS: 1223 ($[M]^+$, 50), 1188 ($[M-Cl]^+$, 15), 905 ($[RuCl(dppm)_2]^+$, 20), 869 ($[Ru(dppm)_2]^+$, 100). Anal. Calc. for $C_{72}H_{68}ClNOP_4Ru$: C, 70.67; H, 5.60; N, 1.14. Found: C, 70.30; H, 5.93; N, 0.92%. UV–vis (λ_{max} nm [ε, M^{-1} cm^{-1}]): 645 [8020], 319 [sh, 18 100], 273 [29 600], 268 [29 400]: IR: ν(C≡C) 2067 cm^{-1}. ^{1}H-NMR: δ 1.27 (s, 9H), 1.31 (s, 9H) (Me_a, Me_b), 4.91 (m, 4H, CH_2), 6.04 (d, 2H, $J_{HH} = 8$ Hz, H_4), 6.53 (d, 2H, $J_{HH} = 8$ Hz, H_5), 6.94 (d, 1H, $J_{HH} = 3$ Hz, H_{10} or H_{14}), 7.02–7.43 (m, 50H, phenyl and H_{14} or H_{10}). ^{31}P-NMR: δ −6.1 (PPh_2). ^{13}C-NMR: δ 29.4 (Me_a, Me_b), 35.3, 35.7 (C_{15}, C_{16}), 50.3 (CH_2), 114.2 (C_2), 122.0 (C_5), 127.5 (C_p), 128.5 (C_3), 129.2 (d, $J_{CP} =$ 23 Hz, C_m), 133.5 (d, $J_{CP} = 23$ Hz, C_o), 134.5 (m, C_i), 130.5 (C_4), 122.2, 135.0 (C_{10}, C_{14}), 144.5 (C_6), 151.8, 152.1, 156.5 (C_9, C_{11}, C_{13}), 187.8 (C_{12}).

3.3.2. [Ru(C≡C-4-C_6H_4N=$\overline{\text{CCH=C}^t\text{BuC(O)C}^t\text{Bu=C}}$H)($PPh_3$)$_2$($\eta$-$C_5H_5$)] (**3**)

[RuCl(PPh_3)$_2$(η-C_5H_5)] (90 mg, 0.12 mmol) and 4-HC≡CC_6H_4N=$\overline{\text{CCH=C}^t\text{BuC(O)C}^t\text{Bu=C}}$H (50 mg, 0.16 mmol) were stirred in methanol (10 ml) at reflux for 45 min. The mixture was then cooled to r.t. and sodium methoxide solution (1 ml, 0.2 M solution in methanol) was added with stirring. The solvent was removed and the residue purified by column chromatography on silica. The product was then recrystallized from dichloromethane–pet. spirit to afford 40 mg (32%) of dark blue microcrystals. FAB MS: 1009 ([M]$^+$, 25), 746 ([M + H − PPh_3]$^+$, 30), 691 ([Ru(PPh_3)$_2$(η-C_5H_5)$^+$, 25), 429 ([Ru(PPh_3)(η-C_5H_5)]$^+$, 100). Anal. Calc. for $C_{63}H_{59}NOP_2Ru$: C, 74.98; H, 5.89; N, 1.39. Found: C, 75.92; H, 5.97; N, 1.12%. UV–vis (λ_{max}, nm [ε, M^{-1} cm^{-1}]): 625 [15 500], 317 [29 800], 239 [34 400]. IR: ν(C≡C) 2061 cm^{-1}. ^{1}H-NMR: δ 1.24 (s, 9H), 1.32 (s, 9H, Me_a, Me_b), 4.32 (s, 5H, C_5H_5), 6.77 (d, 2H, $J_{HH} = 8$ Hz, H_4), 7.01–7.48 (m, 34H, Ph). ^{31}P-NMR: δ 50.7 (PPh_3). ^{13}C-NMR: δ 29.5 (Me_a, Me_b), 35.3, 35.7 (C_{15}, C_{16}), 85.3 (C_5H_5), 115.6 (C_2), 122.5 (C_5), 127.2 (t, $J_{CP} = 5$ Hz, C_m), 128.4 (C_p), 129.1 (C_3), 131.0 (C_4), 133.8 (t, $J_{CP} = 5$ Hz, C_o), 122.1, 135.0 (C_{10}, C_{14}), 138.7 (m, C_i), 145.2 (C_6), 151.9, 152.5, 156.9 (C_9, C_{11}, C_{13}), 187.9 (C_{12}).

3.4. X-ray structural study

A purple plate (0.30 × 0.30 × 0.04 mm^3) grown by diffusion of *n*-heptane into a chloroform solution of **3** was mounted on a glass fiber with oil. Data were collected on a Nonius KappaCCD diffractometer using graphite-monochromated Mo–K_α radiation. A set of ten images were collected and used to determine the cell constants. Data were collected (200 K) as 334 frames via ω-rotation ($\Delta\omega = 0.7°$) with 52 s exposure times. The intensities of 217 072 reflections were collected to 2θmax = 55.0°; equivalent reflections were merged to yield 14 433 unique reflections ($R_{int} = 0.087$). An analytical absorption correction was applied which resulted in transmission factors ranging from 0.888–0.986. Data were corrected for Lorentz and polarization effects. The structure was solved by direct methods (SIR-92), and expanded using difference Fourier techniques. The non-hydrogen atoms were refined with anisotropic displacement by minimising $\Sigma w(|F_o| - |F_c|)^2$ where $w = [\sigma_c^2(F_o) + (p^2/4)F_o^2]^{-1}$, except for those in the solvent molecule which were modelled isotropically. Hydrogen atoms were included in calculated positions but not refined. No hydrogens were included with the heptane solvent molecule. The final cycle of full-matrix least-squares refinement was based on 7320 observed reflections [$I > 3\sigma(I)$] and 641 variable parameters. The maximum and minimum peaks in the final difference Fourier map corresponded to 1.02 and −0.67 e Å^{-3}, respectively, and were found in the region of the disordered heptane molecule (0.5 occupancy). All calculations were performed using the crystallographic software package MAXUS [23] and TEXSAN [24].

3.4.1. Crystal data for $C_{66.5}H_{59}NOP_2Ru$

$M_f = 1051.22$, monoclinic, space group $P2_1/a$, $a = 17.0623(5)$ Å, $b = 18.8222(6)$ Å, $c = 20.4641(7))$ Å, $\beta = 106.482(2)°$, $V = 6302.0(3)$ Å^3, $Z = 4$, $D_{calc} = 1.108$ g cm^{-3}, μ(Mo–K_α) = 3.37 cm^{-1}. $R = \Sigma(|F_o| - |F_c|)/\Sigma(|F_o|) = 0.075$, $R_w[\{\Sigma w(|F_o| - |F_c|)^2\}/\Sigma wF_o^2]^{1/2} = 0.093$, GOF = 2.22.

3.5. Hyper–Rayleigh scattering measurements

An injection-seeded Nd:YAG laser (Q-switched Nd:YAG Quanta Ray GCR5, 1064 nm, 8 ns pulses, 10 Hz) was focussed into a cylindrical cell (7 ml) containing the sample. The intensity of the incident beam was varied by rotation of a half-wave plate placed between crossed polarizers. Part of the laser pulse was sampled by a photodiode to measure the vertically polarized incident light intensity. The frequency doubled light

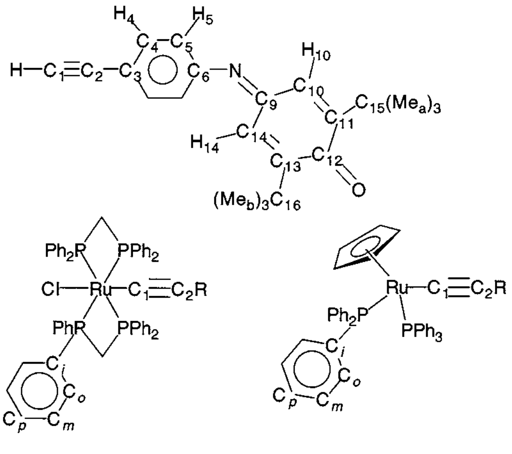

Fig. 3. NMR labeling schemes.

was collected by an efficient condenser system and detected by a photomultiplier. The harmonic scattering and linear scattering were distinguished by appropriate filters; gated integrators were used to obtain intensities of the incident and harmonic scattered light. The absence of luminescence contribution to the harmonic signal was confirmed by using interference filters of different wavelengths near 532 nm. All measurements were performed in tetrahydrofuran using *p*-nitroaniline ($\beta = 21.4 \times 10^{-30}$ esu) [25] as a reference. Solutions were sufficiently dilute that absorption of scattered second-harmonic light was negligible. Further details of the experimental procedure have been reported in the literature [26,27].

4. Supplementary material

Crystallographic data for the structure reported in the paper have been deposited with the Cambridge Crystallographic Data Centre, CCDC no. 141947 for compound **3**. Copies of this information may be obtained free of charge from The Director, CCDC, 12 Union Road, Cambridge, CB2 1EZ, UK (fax: +44-1223-336033; e-mail: deposit@ccdc.cam.ac.uk or www: http://www.ccdc.cam.ac.uk).

Acknowledgements

We thank the Fund for Scientific Research-Flanders (G.0338.98, G.0407.98) (A.P.), the Belgian Government (IUAP-IV/11) (A.P.), the K.U. Leuven (GOA/2000/03) (A.P.), and the Australian Research Council (M.G.H.) for financial support, and Johnson-Matthey Technology Centre for the loan of ruthenium salts (M.G.H.). S.H. is a postdoctoral researcher of the Fund for Scientific Research-Flanders, M.G.H. is an ARC Australian Senior Research Fellow, N.T.L. holds and A.M.M. held an Australian Postgraduate Award.

References

[1] M.P. Cifuentes, J. Driver, M.G. Humphrey, I. Asselberghs, A. Persoons, M. Samoc, B. Luther-Davies, J. Organomet. Chem. (2000) in press.

[2] S.R. Marder, in: D.W. Bruce, D. O'Hare (Eds.), Inorganic Materials, Wiley, New York, 1992, p. 116.

[3] N.J. Long, Angew. Chem. Int. Ed. Engl. 34 (1995) 21.

[4] T. Verbiest, S. Houbrechts, M. Kauranen, K. Clays, A. Persoons, J. Mater. Chem. 7 (1997) 2175.

[5] I.R. Whittall, A.M. McDonagh, M.G. Humphrey, M. Samoc, Adv. Organomet. Chem. 42 (1998) 291.

[6] I.R. Whittall, A.M. McDonagh, M.G. Humphrey, M. Samoc, Adv. Organomet. Chem. 43 (1999) 349.

[7] R.H. Naulty, A.M. McDonagh, I.R. Whittall, M.P. Cifuentes, M.G. Humphrey, S. Houbrechts, J. Maes, A. Persoons, G.A. Heath, D.C.R. Hockless, J. Organomet. Chem. 563 (1998) 137.

[8] S.R. Marder, D.N. Beratan, L.T. Cheng, Science 252 (1991) 103.

[9] S.R. Marder, L.T. Cheng, B.G. Tiemann, J. Chem. Soc. Chem. Commun. (1992) 672.

[10] J. Figueras, P.W. Scullard, A.R. Mack, J. Org. Chem. 36 (1971) 3497.

[11] S. Takahashi, Y. Kuroyama, K. Sonogashira, N. Hagihara, Synthesis (1980) 627.

[12] I.R. Whittall, M.G. Humphrey, A. Persoons, S. Houbrechts, Organonmetallics 15 (1996) 1935.

[13] I.R. Whittall, M.G. Humphrey, S. Houbrechts, A. Persoons, D.C.R. Hockless, Organometallics 15 (1996) 5738.

[14] I.R. Whittall, M.P. Cifuentes, M.G. Humphrey, B. Luther-Davies, M. Samoc, S. Houbrechts, A. Persoons, G.A. Heath, D.C.R. Hockless, J. Organomet. Chem. 549 (1997) 127.

[15] I.R. Whittall, M.P. Cifuentes, M.G. Humphrey, B. Luther-Davies, M. Samoc, S. Houbrechts, A. Persoons, G.A. Heath, D. Bogsanyi, Organometallics 16 (1997) 2631.

[16] D. Touchard, P. Haquette, N. Pirio, L. Toupet, P.H. Dixneuf, Organometallics 12 (1993) 3132.

[17] M.I. Bruce, R.C. Wallis, Aust. J. Chem. 32 (1979) 1471.

[18] I.R. Whittall, M.G. Humphrey, D.C.R. Hockless, B.W. Skelton, A.H. White, Organometallics 14 (1995) 3970.

[19] S. Houbrechts, K. Clays, A. Persoons, V. Cadierno, M.P. Gamasa, J. Gimeno, I.R. Whittall, M.G. Humphrey, Proc. SPIE-Int. Soc. Opt. Eng. 2852 (1996) 98.

[20] A.M. McDonagh, I.R. Whittall, M.G. Humphrey, B.W. Skelton, A.H. White, J. Organomet. Chem. 519 (1996) 229.

[21] M.I. Bruce, C. Hamiester, A.G. Swincer, R.C. Wallis, Inorg. Synth. 21 (1982) 78.

[22] B. Chaudret, G. Commenges, R. Poiblanc, J. Chem. Soc. Dalton Trans. (1984) 1635.

[23] S. Mackay, C.J. Gilmore, C. Edwards, M. Tremayne, N. Stuart, K. Shankland, MAXUS Computer Program for the Solution and Refinement of Crystal Structures, Nonius, The Netherlands; MacScience, Japan; The University of Glasgow, 2000.

[24] TEXSAN: Single Crystal Structure Analysis Package, Molecular Structure Corporation, The Woodlands, TX, 1997.

[25] M. Stähelin, D.M. Burland, J.E. Rice, Chem. Phys. Lett. 191 (1992) 245.

[26] K. Clays, A. Persoons, Rev. Sci. Instrum. 63 (1992) 3285.

[27] S. Houbrechts, K. Clays, A. Persoons, Z. Pikramenou, J.-M. Lehn, Chem. Phys. Lett. 258 (1996) 485.